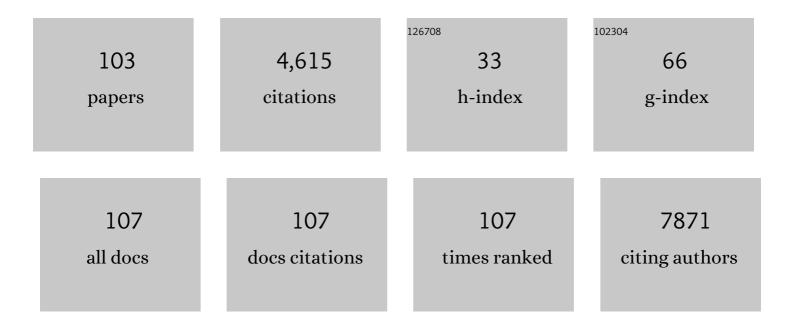
David J Lewis

List of Publications by Year in descending order

Source: https://exaly.com/author-pdf/454616/publications.pdf Version: 2024-02-01



| # | Article | IF | CITATIONS |
|----|---|-----|-----------|
| 1 | Production of few-layer phosphorene by liquid exfoliation of black phosphorus. Chemical Communications, 2014, 50, 13338-13341. | 2.2 | 667 |
| 2 | Synthesis, Properties, and Applications of Transition Metal-Doped Layered Transition Metal Dichalcogenides. Chemistry of Materials, 2016, 28, 1965-1974. | 3.2 | 424 |
| 3 | Highly Luminescent, Triple- and Quadruple-Stranded, Dinuclear Eu, Nd, and Sm(III) Lanthanide Complexes Based on Bis-Diketonate Ligands. Journal of the American Chemical Society, 2004, 126, 9413-9424. | 6.6 | 339 |
| 4 | Tin(II) Sulfide (SnS) Nanosheets by Liquid-Phase Exfoliation of Herzenbergite: IV–VI Main Group Two-Dimensional Atomic Crystals. Journal of the American Chemical Society, 2015, 137, 12689-12696. | 6.6 | 220 |
| 5 | Nanostructured Aptamer-Functionalized Black Phosphorus Sensing Platform for Label-Free Detection of Myoglobin, a Cardiovascular Disease Biomarker. ACS Applied Materials & Interfaces, 2016, 8, 22860-22868. | 4.0 | 208 |
| 6 | Fully printed high performance humidity sensors based on two-dimensional materials. Nanoscale, 2018, 10, 5599-5606. | 2.8 | 142 |
| 7 | Luminescent nanobeads: attachment of surface reactive Eu(iii) complexes to gold nanoparticles. Chemical Communications, 2006, , 1433. | 2.2 | 126 |
| 8 | Purely Heterometallic Lanthanide(III) Macrocycles through Controlled Assembly of Disulfide Bonds for Dual Color Emission. Journal of the American Chemical Society, 2011, 133, 1033-1043. | 6.6 | 103 |
| 9 | On the interaction of copper(<scp>ii</scp>) with disulfiram. Chemical Communications, 2014, 50, 13334-13337. | 2.2 | 92 |
| 10 | Routes to tin chalcogenide materials as thin films or nanoparticles: a potentially important class of semiconductor for sustainable solar energy conversion. Inorganic Chemistry Frontiers, 2014, 1, 577-598. | 3.0 | 87 |
| 11 | Ambient-air-stable inorganic Cs ₂ Snl ₆ double perovskite thin films <i>via</i> aerosol-assisted chemical vapour deposition. Journal of Materials Chemistry A, 2018, 6, 11205-11214. | 5.2 | 85 |
| 12 | Shining a light on transition metal chalcogenides for sustainable photovoltaics. Chemical Science, 2017, 8, 4177-4187. | 3.7 | 84 |
| 13 | pH-controlled delivery of luminescent europium coated nanoparticles into platelets. Proceedings of the United States of America, 2012, 109, 1862-1867. | 3.3 | 78 |
| 14 | Thin Films of Molybdenum Disulfide Doped with Chromium by Aerosol-Assisted Chemical Vapor Deposition (AACVD). Chemistry of Materials, 2015, 27, 1367-1374. | 3.2 | 78 |
| 15 | In situ investigation of degradation at organometal halide perovskite surfaces by X-ray photoelectron spectroscopy at realistic water vapour pressure. Chemical Communications, 2017, 53, 5231-5234. | 2.2 | 78 |
| 16 | Ambient pressure aerosol-assisted chemical vapour deposition of (CH ₃ NH ₃)PbBr ₃ , an inorganic–organic perovskite important in photovoltaics. Chemical Communications, 2014, 50, 6319-6321. | 2.2 | 75 |
| 17 | Thin films of tin(II) sulphide (SnS) by aerosol-assisted chemical vapour deposition (AACVD) using tin(II) dithiocarbamates as single-source precursors. Journal of Crystal Growth, 2015, 415, 93-99. | 0.7 | 75 |
| 18 | Solution processing of two-dimensional black phosphorus. Chemical Communications, 2017, 53, 1445-1458. | 2.2 | 63 |

| # | Article | IF | CITATIONS |
|----|--|-----|-----------|
| 19 | Transition metal doped pyrite (FeS ₂) thin films: structural properties and evaluation of optical band gap energies. Journal of Materials Chemistry C, 2015, 3, 12068-12076. | 2.7 | 59 |
| 20 | Bis(piperidinedithiocarbamato)pyridinecadmium(<scp>ii</scp>) as a single-source precursor for the synthesis of CdS nanoparticles and aerosol-assisted chemical vapour deposition (AACVD) of CdS thin films. New Journal of Chemistry, 2014, 38, 6073-6080. | 1.4 | 55 |
| 21 | De Novo Design of Ln(III) Coiled Coils for Imaging Applications. Journal of the American Chemical Society, 2014, 136, 1166-1169. | 6.6 | 55 |
| 22 | Mechanical Properties of Molybdenum Disulfide and the Effect of Doping: An in Situ TEM Study. ACS Applied Materials & Interfaces, 2015, 7, 20829-20834. | 4.0 | 50 |
| 23 | Heterocyclic dithiocarbamato-iron(<scp>iii</scp>) complexes: single-source precursors for aerosol-assisted chemical vapour deposition (AACVD) of iron sulfide thin films. Dalton Transactions, 2016, 45, 2647-2655. | 1.6 | 49 |
| 24 | Chemical vapour deposition of rhenium disulfide and rhenium-doped molybdenum disulfide thin films using single-source precursors. Journal of Materials Chemistry C, 2016, 4, 2312-2318. | 2.7 | 46 |
| 25 | Supercapacitor Electrodes from the in Situ Reaction between Two-Dimensional Sheets of Black Phosphorus and Graphene Oxide. ACS Applied Materials & Interfaces, 2018, 10, 10330-10338. | 4.0 | 44 |
| 26 | Sequential bottom-up and top-down processing for the synthesis of transition metal dichalcogenide nanosheets: the case of rhenium disulfide (ReS ₂). Chemical Communications, 2016, 52, 7878-7881. | 2.2 | 42 |
| 27 | Synthesis of pyrite thin films and transition metal doped pyrite thin films by aerosol-assisted chemical vapour deposition. New Journal of Chemistry, 2015, 39, 1013-1021. | 1.4 | 41 |
| 28 | Exploring the versatility of liquid phase exfoliation: producing 2D nanosheets from talcum powder, cat litter and beach sand. 2D Materials, 2017, 4, 025054. | 2.0 | 39 |
| 29 | Direct synthesis of MoS ₂ or MoO ₃ <i>via</i> thermolysis of a dialkyl dithiocarbamato molybdenum(<scp>iv</scp>) complex. Chemical Communications, 2019, 55, 99-102. | 2.2 | 38 |
| 30 | A Review of the Synthesis, Properties, and Applications of Bulk and Two-Dimensional Tin (II) Sulfide (SnS). Applied Sciences (Switzerland), 2021, 11, 2062. | 1.3 | 37 |
| 31 | Lanthanide-coated gold nanoparticles for biomedical applications. Coordination Chemistry Reviews, 2014, 273-274, 213-225. | 9.5 | 36 |
| 32 | Intracellular synchrotron nanoimaging and DNA damage/genotoxicity screening of novel lanthanide-coated nanovectors. Nanomedicine, 2010, 5, 1547-1557. | 1.7 | 35 |
| 33 | On the stability of surfactant-stabilised few-layer black phosphorus in aqueous media. RSC Advances, 2016, 6, 86955-86958. | 1.7 | 35 |
| 34 | Formation and Healing of Defects in Atomically Thin GaSe and InSe. ACS Nano, 2019, 13, 5112-5123. | 7.3 | 35 |
| 35 | Updating the road map to metal-halide perovskites for photovoltaics. Journal of Materials Chemistry A, 2017, 5, 17135-17150. | 5.2 | 33 |
| 36 | Evaluation of quinoline as a remote sensitiser for red and near-infrared emissive lanthanide(iii) ions in solution and the solid state. Dalton Transactions, 2012, 41, 13138. | 1.6 | 31 |

| # | Article | IF | CITATIONS |
|----|---|-----|-----------|
| 37 | High entropy metal chalcogenides: synthesis, properties, applications and future directions. Chemical Communications, 2022, 58, 8025-8037. | 2.2 | 31 |
| 38 | Scalable and Universal Route for the Deposition of Binary, Ternary, and Quaternary Metal Sulfide Materials from Molecular Precursors. ACS Applied Energy Materials, 2020, 3, 1952-1961. | 2.5 | 30 |
| 39 | Single-Source Precursor for Tungsten Dichalcogenide Thin Films: Mo _{1–<i>x</i>} W _{<i>x</i>} S ₂ (0 ≤i>x ≤) Alloys by Aerosol-Assisted Chemical Vapor Deposition. Chemistry of Materials, 2017, 29, 3858-3862. | 3.2 | 28 |
| 40 | Black phosphorus with near-superhydrophobic properties and long-term stability in aqueous media. Chemical Communications, 2018, 54, 3831-3834. | 2.2 | 28 |
| 41 | A molecular precursor route to quaternary chalcogenide CFTS (Cu2FeSnS4) powders as potential solar absorber materials. RSC Advances, 2019, 9, 24146-24153. | 1.7 | 28 |
| 42 | Renewable Adsorbent for the Separation of Surfactant-Stabilized Oil in Water Emulsions Based on Nanostructured Sawdust. ACS Sustainable Chemistry and Engineering, 2019, 7, 18935-18942. | 3.2 | 28 |
| 43 | Flexible nanoporous activated carbon for adsorption of organics from industrial effluents. Nanoscale, 2021, 13, 15311-15323. | 2.8 | 26 |
| 44 | A Freeâ€Standing and Selfâ€Healable 2D Supramolecular Material Based on Hydrogen Bonding: A Nanowire Array with Subâ€2â€nm Resolution. Small, 2017, 13, 1604077. | 5.2 | 24 |
| 45 | Chemical vapor deposition of tin sulfide from diorganotin(IV) dixanthates. Journal of Materials Science, 2019, 54, 2315-2323. | 1.7 | 24 |
| 46 | Bioinspired scaffolds that sequester lead ions in physically damaged high efficiency perovskite solar cells. Chemical Communications, 2021, 57, 994-997. | 2.2 | 24 |
| 47 | Dual Functionalization of Liquidâ€Exfoliated Semiconducting 2 <i>Hâ€</i> MoS ₂ with Lanthanide Complexes Bearing Magnetic and Luminescence Properties. Advanced Functional Materials, 2017, 27, 1703646. | 7.8 | 23 |
| 48 | Synthesis of Bi _{2â^2x} Sb _{2x} S ₃ (O ≤i>x ≤) solid solutions from solventless thermolysis of metal xanthate precursors. Journal of Materials Chemistry C, 2018, 6, 12652-12659. | 2.7 | 23 |
| 49 | Synthesis of nanostructured powders and thin films of iron sulfide from molecular precursors. RSC Advances, 2018, 8, 29096-29103. | 1.7 | 21 |
| 50 | Silica Nanoparticles for Micro-Particle Imaging Velocimetry: Fluorosurfactant Improves Nanoparticle Stability and Brightness of Immobilized Iridium(III) Complexes. Langmuir, 2013, 29, 14701-14708. | 1.6 | 18 |
| 51 | Morphology and band gap controlled AACVD of CdSe and CdS Se1â~' thin films using novel single source precursors: Bis(diethyldithio/diselenocarbamato)cadmium(II). Materials Science in Semiconductor Processing, 2015, 40, 848-854. | 1.9 | 18 |
| 52 | The influence of precursor on rhenium incorporation into Re-doped MoS ₂ (Mo _{1â^'x} Re _x S ₂) thin films by aerosol-assisted chemical vapour deposition (AACVD). Journal of Materials Chemistry C, 2017, 5, 9044-9052. | 2.7 | 18 |
| 53 | On the phase control of CuInS ₂ nanoparticles from Cu-/In-xanthates. Dalton Transactions, 2018, 47, 5304-5309. | 1.6 | 16 |
| 54 | Room-Temperature Production of Nanocrystalline Molybdenum Disulfide (MoS ₂) at the Liquidâ^²Liquid Interface. Chemistry of Materials, 2019, 31, 5384-5391. | 3.2 | 16 |

| # | Article | IF | CITATIONS |
|----|--|-----|-----------|
| 55 | Synthetic 2-D lead tin sulfide nanosheets with tuneable optoelectronic properties from a potentially scalable reaction pathway. Chemical Science, 2019, 10, 1035-1045. | 3.7 | 16 |
| 56 | Synthesis of ternary copper antimony sulfide via solventless thermolysis or aerosol assisted chemical vapour deposition using metal dithiocarbamates. Scientific Reports, 2022, 12, 5627. | 1.6 | 16 |
| 57 | Synthesis of High Entropy Lanthanide Oxysulfides via the Thermolysis of a Molecular Precursor Cocktail. Journal of the American Chemical Society, 2021, 143, 21560-21566. | 6.6 | 16 |
| 58 | Property Self-Optimization During Wear of MoS ₂ . ACS Applied Materials & Interfaces, 2017, 9, 1953-1958. | 4.0 | 15 |
| 59 | High magnetic relaxivity in a fluorescent CdSe/CdS/ZnS quantum dot functionalized with MRI contrast molecules. Chemical Communications, 2017, 53, 10500-10503. | 2.2 | 14 |
| 60 | Exploiting Inherent Instability of 2D Black Phosphorus for Controlled Phosphate Release from Blow-Spun Poly(lactide- <i>co</i> -glycolide) Nanofibers. ACS Applied Nano Materials, 2018, 1, 4190-4197. | 2.4 | 14 |
| 61 | Surface Engineering of Ceramic Nanomaterials for Separation of Oil/Water Mixtures. Frontiers in Chemistry, 2020, 8, 578. | 1.8 | 14 |
| 62 | Direct synthesis of nanostructured silver antimony sulfide powders from metal xanthate precursors. Scientific Reports, 2021, 11, 3053. | 1.6 | 14 |
| 63 | Diatom Frustules as a Biomineralized Scaffold for the Growth of Molybdenum Disulfide Nanosheets. Chemistry of Materials, 2016, 28, 5582-5586. | 3.2 | 13 |
| 64 | Air-Stable Methylammonium Lead Iodide Perovskite Thin Films Fabricated via Aerosol-Assisted Chemical Vapor Deposition from a Pseudohalide Pb(SCN) ₂ Precursor. ACS Applied Energy Materials, 2019, 2, 6012-6022. | 2.5 | 13 |
| 65 | Rapid and Low-Temperature Molecular Precursor Approach toward Ternary Layered Metal Chalcogenides and Oxides: Mo _{1–<i>x</i>} W _{<i>x</i>} S ₂ and Mo _{1–<i>x</i>} W _{<i>x</i>} O ₃ Alloys (O ≤i>x ≤). Chemistry of Materials, 2020, 32, 7895-7907. | 3.2 | 13 |
| 66 | Scalable synthesis of Cu–Sb–S phases from reactive melts of metal xanthates and effect of cationic manipulation on structural and optical properties. Scientific Reports, 2021, 11, 1887. | 1.6 | 13 |
| 67 | Luminescent Gold Surfaces for Sensing and Imaging: Patterning of Transition Metal Probes. ACS Applied Materials & Interfaces, 2014, 6, 11598-11608. | 4.0 | 12 |
| 68 | Tailoring iridium luminescence and gold nanoparticle size for imaging of microvascular blood flow. Nanomedicine, 2017, 12, 2725-2740. | 1.7 | 12 |
| 69 | Nanoscale Chevrel-Phase Mo ₆ S ₈ Prepared by a Molecular Precursor Approach for Highly Efficient Electrocatalysis of the Hydrogen Evolution Reaction in Acidic Media. ACS Applied Energy Materials, 2021, 4, 13015-13026. | 2.5 | 12 |
| 70 | Important Phase Control of Indium Sulfide Nanomaterials by Choice of Indium(III) Xanthate Precursor and Thermolysis Temperature. European Journal of Inorganic Chemistry, 2019, 2019, 1421-1432. | 1.0 | 11 |
| 71 | New insights into polymer mediated formation of anatase mesocrystals. CrystEngComm, 2017, 19, 3281-3287. | 1.3 | 10 |
| 72 | Molecular Precursor Route to Bournonite (CuPbSbS ₃) Thin Films and Powders. Inorganic Chemistry, 2021, 60, 13691-13698. | 1.9 | 10 |

| # | Article | IF | CITATIONS |
|----|---|-----|-----------|
| 73 | Decoupling Structure and Composition of CH ₃ NH ₃ Pbl _{3–<i>x</i>} Br _{<i>x</i>} Films Prepared by Combined One-Step and Two-Step Deposition. ACS Applied Energy Materials, 2018, 1, 5567-5578. | 2.5 | 9 |
| 74 | Intrinsic effects of thickness, surface chemistry and electroactive area on nanostructured MoS2 electrodes with superior stability for hydrogen evolution. Electrochimica Acta, 2021, 382, 138257. | 2.6 | 9 |
| 75 | High-Performance Nanostructured MoS ₂ Electrodes with Spontaneous Ultralow Gold Loading for Hydrogen Evolution. Journal of Physical Chemistry C, 2021, 125, 20940-20951. | 1.5 | 9 |
| 76 | Nanocubes of Mo ₆ S ₈ Chevrel phase as active electrode material for aqueous lithium-ion batteries. Nanoscale, 2022, 14, 10125-10135. | 2.8 | 9 |
| 77 | Full compositional control of PbS _x Se _{1â°x} thin films by the use of acylchalcogourato lead(<scp>ii</scp>) complexes as precursors for AACVD. Dalton Transactions, 2018, 47, 16938-16943. | 1.6 | 8 |
| 78 | Chemical vapour deposition of chromium-doped tungsten disulphide thin films on glass and steel substrates from molecular precursors. Journal of Materials Chemistry C, 2018, 6, 9537-9544. | 2.7 | 8 |
| 79 | Accessing γ-Ga ₂ S ₃ by solventless thermolysis of gallium xanthates: a low-temperature limit for crystalline products. Dalton Transactions, 2019, 48, 15605-15612. | 1.6 | 8 |
| 80 | Solid solutions of M _{2â^'2x} In _{2x} S ₃ (M = Bi or Sb) by solventless thermolysis. Journal of Materials Chemistry C, 2019, 7, 5112-5121. | 2.7 | 8 |
| 81 | A novel and potentially scalable CVD-based route towards SnO2:Mo thin films as transparent conducting oxides. Journal of Materials Science, 2021, 56, 15921-15936. | 1.7 | 8 |
| 82 | Tunable structural and optical properties of CuInS2 colloidal quantum dots as photovoltaic absorbers. RSC Advances, 2021, 11, 21351-21358. | 1.7 | 8 |
| 83 | Controlled assembly of heterometallic lanthanide(III) macrocycles: incorporation of photoactive and highly paramagnetic metal centres within a single complex. Supramolecular Chemistry, 2012, 24, 135-142. | 1.5 | 7 |
| 84 | Heterometallic 3d–4f Complexes as Air-Stable Molecular Precursors in Low Temperature Syntheses of Stoichiometric Rare-Earth Orthoferrite Powders. Inorganic Chemistry, 2020, 59, 15796-15806. | 1.9 | 7 |
| 85 | Luminescent ruthenium(II) tris-bipyridyl complex caged in nanoscale silica for particle velocimetry studies in microchannels. Measurement Science and Technology, 2012, 23, 084004. | 1.4 | 6 |
| 86 | Optimization of superhydrophobicity at the surface of iron sulfide thin films by a wet chemical approach. Materials Research Bulletin, 2021, 144, 111476. | 2.7 | 6 |
| 87 | Thin films of formamidinium lead iodide (FAPI) deposited using aerosol assisted chemical vapour deposition (AACVD). Scientific Reports, 2020, 10, 22245. | 1.6 | 6 |
| 88 | Investigating the Effect of Steric Hindrance within CdS Single-Source Precursors on the Material Properties of AACVD and Spin-Coat-Deposited CdS Thin Films. Inorganic Chemistry, 2022, 61, 8206-8216. | 1.9 | 6 |
| 89 | Synthesis of iron sulfide thin films and powders from new xanthate precursors. Journal of Crystal Growth, 2019, 522, 175-182. | 0.7 | 5 |
| 90 | Preparation of solution processed photodetectors comprised of two-dimensional tin(<scp>ii</scp>) sulfide nanosheet thin films assembled <i>via</i> the Langmuir–Blodgett method. RSC Advances, 2021, 11, 26813-26819. | 1.7 | 5 |

| # | Article | IF | CITATIONS |
|-----|--|-----|-----------|
| 91 | Synthesis, X-ray Single-Crystal Structural Characterization, and Thermal Analysis of Bis(O-alkylxanthato)Cd(II) and Bis(O-alkylxanthato)Zn(II) Complexes Used as Precursors for Cadmium and Zinc Sulfide Thin Films. Inorganic Chemistry, 2021, 60, 7573-7583. | 1.9 | 5 |
| 92 | Tunable structural, morphological and optical properties of undoped, Mn, Ni and Ag-doped CuInS2 thin films prepared by AACVD. Materials Science in Semiconductor Processing, 2022, 137, 106224. | 1.9 | 5 |
| 93 | Synthesis of molybdenum-doped rhenium disulfide alloy using aerosol-assisted chemical vapour deposition. Materials Science in Semiconductor Processing, 2021, 127, 105718. | 1.9 | 4 |
| 94 | Paul O'Brien: Materials Chemistry Pioneer (Jan 22, 1954–Oct 16, 2018). Chemistry of Materials, 2018, 30, 8113-8115. | 3.2 | 3 |
| 95 | Synthesis of indium oxide microparticles using aerosol assisted chemical vapour deposition. RSC Advances, 2020, 10, 22487-22490. | 1.7 | 3 |
| 96 | Testing the Efficacy of the Synthesis of Iron Antimony Sulfide Powders from Single Source Precursors. Inorganics, 2021, 9, 61. | 1.2 | 3 |
| 97 | Structural Investigations of α-MnS Nanocrystals and Thin Films Synthesized from Manganese(II) Xanthates by Hot Injection, Solvent-Less Thermolysis, and Doctor Blade Routes. ACS Omega, 2021, 6, 27716-27725. | 1.6 | 3 |
| 98 | Sustainable ITO films with reduced indium content deposited by AACVD. Journal of Materials Chemistry C, 2022, 10, 579-589. | 2.7 | 3 |
| 99 | Ricinoleic Acid as a Green Alternative to Oleic Acid in the Synthesis of Doped Nanocrystals. ChemistrySelect, 2018, 3, 13548-13552. | 0.7 | 2 |
| 100 | Paul O'Brien. 22 January 1954—16 October 2018. Biographical Memoirs of Fellows of the Royal Society, 2020, 69, 443-466. | 0.1 | 2 |
| 101 | A review of two-dimensional nanomaterials beyond graphene. SPR Nanoscience, 0, , 108-141. | 0.3 | 2 |
| 102 | Formation and Characterization of Model Iron Sulfide Scales with Disulfides and Thiols on Steel Pipeline Materials by an Aerosol-Assisted Chemical Vapor Method. Energy & Fuels, 2017, 31, 2496-2500. | 2.5 | 0 |
| 103 | Biological applications of nanomaterials. SPR Nanoscience, 2016, , 276-323. | 0.3 | 0 |